

Selectivity of Thiolate Ligand and Preference of Substrate in Model Reactions of Dissimilatory Nitrate Reductase[†]

Amit Majumdar, Kuntal Pal, and Sabyasachi Sarkar*

Department of Chemistry, IIT Kanpur, Kanpur 208016, India

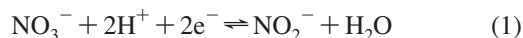
Received December 17, 2007

Complexes analogous to the active site of dissimilatory nitrate reductase from *Desulfovibrio desulfuricans* are synthesized. The hexacoordinated complexes $[\text{PPh}_4][\text{Mo}^{\text{IV}}(\text{PPh}_3)(\text{SR})(\text{mnt})_2]$ ($\text{R} = -\text{CH}_2\text{CH}_3$ (**1**), $-\text{CH}_2\text{Ph}$ (**2**)) released PPh_3 in solution to generate the active model cofactor, $\{\text{Mo}^{\text{IV}}(\text{SR})(\text{mnt})_2\}^{1-}$, ready with a site for nitrate binding. Kinetics for nitrate reduction by the complexes **1** and **2** followed Michaelis–Menten saturation kinetics with a faster rate in the case of **1** ($V_{\text{Max}} = 3.2 \times 10^{-2} \text{ s}^{-1}$, $K_{\text{M}} = 2.3 \times 10^{-4} \text{ M}$) than that reported earlier ($V_{\text{Max}} = 4.2 \times 10^{-3} \text{ s}^{-1}$, $K_{\text{M}} = 4.3 \times 10^{-4} \text{ M}$) (Majumdar, A.; Pal, K.; Sarkar, S. *J. Am. Chem. Soc.* 2006, 128, 4196–4197). The oxidized molybdenum species may be reduced back by PPh_3 to the starting complex, and a catalytic cycle involving $[\text{Bu}_4\text{N}][\text{NO}_3]$ and PPh_3 as the oxidizing and reducing substrates, respectively, is established with the complexes **1** and **2**. Isostructural complexes, $[\text{Et}_4\text{N}][\text{Mo}^{\text{IV}}(\text{PPh}_3)(\text{X})(\text{mnt})_2]$ ($\text{X} = -\text{Br}$ (**3**), $-\text{I}$ (**4**)) did not show any reductive activity toward nitrate. The selectivity of the thiolate ligand for the functional activity and the cessation of such activity in isostructural halo complexes demonstrate the necessity of thiolate coordination. Electrochemical data of all these complexes correlate the ability of the thiolated species for such oxotransfer activity. Compounds **1** and **2** are capable of reducing substrates like TMANO or DMSO, but after the initial 15–20% conversion, the product trimethylamine or dimethylsulfide formed interacts with the active parent complexes **1** and **2** thereby slowing down further oxo-transfer reaction similar to feedback type reactions. From the functional nitrate reduction, the molybdenum species finally reacts with the nitrite formed leading to nitrosylation similar to the NO evolution reaction by periplasmic nitrate reductase from *Pseudomonas denitrificans*. All these complexes (**1–4**) are characterized structurally by X-ray, elemental analysis, electrochemistry, electronic, FT-IR, mass and ³¹P NMR spectroscopic measurements.

Introduction

Under Hille classification¹ of molybdenum oxotransferase enzymes, the DMSOR (dimethylsulfoxide reductase) family conserves two pterin dithiolene (S_2Pd)² moieties and one protein-derived ligand which normally varies with the Ser.O^- , Cys.S^- , or Cys.Se^- residue in their cofactor. In addition to DMSOR and TMANOR (trimethylamine N-oxide reductase), the DMSOR family includes dissimilatory nitrate reductase.¹ This nitrate reductase catalyzes the reduction of nitrate to nitrite (Figure 1) and is found in certain bacteria having the ability to grow on nitrate and use it for their respiration. In dissimilatory nitrate reductase (NiR)² from

Desulfovibrio desulfuricans, the oxidized active site has been structurally characterized as $[\text{Mo}^{\text{VI}}(\text{OH}_x)(\text{S.Cys})(\text{S}_2\text{Pd})_2]$ ($x = 1$ or 2) by X-ray crystallography,³ and the reduced desoxo site $[\text{Mo}^{\text{IV}}(\text{S.Cys})(\text{S}_2\text{Pd})_2]$ has been proposed to mediate the important oxotransfer reaction (eq 1).



It has been proposed³ that nitrate is first bound to the molybdenum center of the reduced cofactor with the formation of an enzyme–substrate complex, followed by the essential oxotransfer and the elimination of the nitrite ion with the formation of oxidized molybdenum cofactor, $[\text{Mo}^{\text{VI}}(\text{O})(\text{S.Cys})(\text{S}_2\text{Pd})_2]$. This oxo form is believed to be very protophilic, resulting in the formation of protonated

[†] Dedicated in the memory of Prof. Edward I. Stiefel.

* To whom correspondence should be addressed. E-mail: abya@iitk.ac.in.

(1) Hille, R. *Chem. Rev.* 1996, 96, 2757–2816.

(2) Abbreviations are given in Chart 1.

(3) Dias, J. M.; Than, M. E.; Humm, A.; Huber, R.; Bourenkov, G. P.; Bartunik, H. D.; Bursakov, S.; Calvete, J.; Caldeira, J.; Carneiro, C.; Moura, J. J.G.; Moura, I.; Romao, M. J. *Structure* 1999, 7, 65–79.

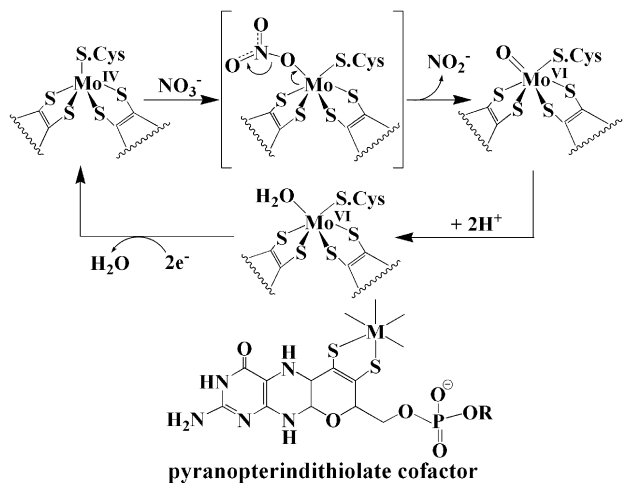


Figure 1. Description of the reduced and oxidized sites of dissimilatory nitrate reductase (*Desulfovibrio desulfuricans*) and the proposed reaction pathway. Also shown is the pyranopterindithiolate cofactor (R is absent or a nucleotide).

oxidized species $[\text{Mo}^{\text{VI}}(\text{OH})_2(\text{S.Cys})(\text{S}_2\text{Pd})_2]$ ($x = 1$ or 2).³ To understand the role of the varied protein derived ligands precisely, molybdoenzymes of the DMSOR family are studied by site-directed mutagenesis.⁴ It is known that this protein–ligand attached to molybdenum in an active site mainly controls the specificity of the active site toward a substrate because the replacement of protein–ligand serinate (in DMSOR²) by cysteinylate or by selenocysteinylate changes the properties of the enzymes along with their activity. The structure of a second dissimilatory nitrate reductase from *Escherichia coli* has been crystallographically established⁵ which contains a $[\text{Mo}^{\text{IV}}(\text{O}_2\text{C.Asp})(\text{S}_2\text{Pd})_2]$ site with an unsymmetrically coordinated carboxylate group.

Nitrate reduction by Mo(IV) complexes devoid of any dithiolene coordination is well-known.⁶ Pentacoordinated molybdenum(IV) bis(dithiolene) monothiolate complexes with resemblance to the active site of NiR have been reported,⁷ which with nitrate^{7a} underwent decomposition⁸ to $[\text{Mo}^{\text{V}}(\text{S}_2\text{C}_2\text{Me}_2)_3]^{1-}$. However, the corresponding tungsten complex was shown to reduce nitrate with a second-order reaction kinetics.⁸ In an attempt to show $[\text{Mo}^{\text{IV}}(\text{SPh})(\text{S}_2\text{C}_2\text{Me}_2)_2]^{1-}$ as the active model cofactor, the irradiation on the hexacoordinated complex, $[\text{Mo}^{\text{IV}}(\text{CO})(\text{SPh})(\text{S}_2\text{C}_2\text{Me}_2)_2]^{1-}$ to remove CO resulted in decomposition^{7a} forming $[\text{Mo}^{\text{V}}(\text{S}_2\text{C}_2\text{Me}_2)_3]^{1-}$. Following the success of the 1,2-dicyanoethylenedithiolate (mnt^{2-})⁹ ligand in the synthesis of the Mo(VI) complex to perform the functional analogue reaction of sulfite oxidase,¹⁰ we used this ligand for the synthesis of desoxo complexes in relevance to NiR.

(4) Hilton, J. C.; Temple, C. A.; Rajagopalan, K. V. *J. Biol. Chem.* **1999**, *274*, 8428.

(5) Bertero, M. G.; Rothery, R. A.; Palak, M.; Hou, C.; Lim, D.; Blasco, F.; Weiner, J. H.; Strynadka, N. C. *J. Nat. Struct. Biol.* **2003**, *10*, 681–687.

(6) (a) Berg, J. M.; Holm, R. H. *J. Am. Chem. Soc.* **1985**, *107*, 925–932. (b) Craig, J. A.; Holm, R. H. *J. Am. Chem. Soc.* **1989**, *111*, 2111–2115.

(7) (a) Lim, B. S.; Donahue, J. P.; Holm, R. H. *Inorg. Chem.* **2000**, *39*, 263–273. (b) Musgrave, K. B.; Lim, B. S.; Sung, K.-M.; Holm, R. H.; Hedman, B.; Hodgson, K. O. *Inorg. Chem.* **2000**, *39*, 5238–5247. (c) Lim, B. S.; Holm, R. H. *J. Am. Chem. Soc.* **2001**, *123*, 1920–1930.

(8) Jiang, J.; Holm, R. H. *Inorg. Chem.* **2005**, *44*, 1068–1072.

Chart 1. Designation of Complexes and Abbreviations

$[\text{PPh}_4][\text{Mo}^{\text{IV}}(\text{PPh}_3)(\text{SCH}_2\text{CH}_3)(\text{mnt})_2] \cdot \text{CH}_2\text{Cl}_2$	1
$[\text{PPh}_4][\text{Mo}^{\text{IV}}(\text{PPh}_3)(\text{SCH}_2\text{Ph})(\text{mnt})_2]$	2
$[\text{Et}_4\text{N}][\text{Mo}^{\text{IV}}(\text{PPh}_3)(\text{Br})(\text{mnt})_2]$	3
$[\text{Et}_4\text{N}][\text{Mo}^{\text{IV}}(\text{PPh}_3)(\text{I})(\text{mnt})_2] \cdot \text{CH}_2\text{Cl}_2$	4
$[\text{Et}_4\text{N}][\text{Mo}^{\text{IV}}(\text{PPh}_3)(\text{SPh})(\text{mnt})_2] \cdot \text{CH}_2\text{Cl}_2$	5¹¹
$[\text{Et}_4\text{N}][\text{Mo}^{\text{IV}}(\text{PPh}_3)(\text{Cl})(\text{mnt})_2] \cdot \text{CH}_2\text{Cl}_2$	6¹¹

NiR, nitrate reductase; S₂pd, pyranopterindithiolate; TMANO, trimethylamine

N – oxide; DMSO, dimethylsulfoxide.

A preliminary study on this functional analogue reaction has been reported.¹¹ To mimic cysteinyl thiolate coordination of the native protein,³ we now refined our study by synthesizing molybdenum(IV) bis(dithiolene) complexes (Chart 1) containing simple aliphatic thiolates. The complexes, $[\text{PPh}_4][\text{Mo}^{\text{IV}}(\text{PPh}_3)(\text{SCH}_2\text{CH}_3)(\text{mnt})_2] \cdot \text{CH}_2\text{Cl}_2$ (**1**) and $[\text{PPh}_4][\text{Mo}^{\text{IV}}(\text{PPh}_3)(\text{SCH}_2\text{Ph})(\text{mnt})_2]$ (**2**) reduce nitrate to nitrite. Kinetics investigation of the reaction using $[\text{Bu}_4\text{N}][\text{NO}_3]$ as the source of nitrate revealed enzymatic saturation kinetics behavior by following Michaelis–Menten kinetics. Compounds **1**, **2**, and **5** (Chart 1) are capable of reducing TMANO or DMSO, but in the case of DMSO, the initial oxo transfer reaction was inhibited by the accumulated reaction product, dimethylsulfide, by blocking the substrate binding site for further reaction, which is similar to feedback inhibition. In the case of the TMANO reduction, the product trimethylamine, being basic, combines with the trace amount of moisture present even in dry solvent and thereby decomposes the active species responsible for TMANO reduction. The formation of DMS-coordinated complexes of **1**, **2**, or **5** can be monitored spectroscopically, but these could not be isolated because they are unstable; this led to the formation of stable tris-dithiolene complexes. Complexes $[\text{Et}_4\text{N}][\text{Mo}^{\text{IV}}(\text{PPh}_3)(\text{Br})(\text{mnt})_2]$ (**3**) and $[\text{Et}_4\text{N}][\text{Mo}^{\text{IV}}(\text{PPh}_3)(\text{I})(\text{mnt})_2]$ (**4**), isostructural to **1** and **2**, have been synthesized to compare their ability to participate in similar oxo transfer reactions. However, these complexes do not show any reductive activity toward nitrate, TMANO, or DMSO. The inability to isolate the oxidized complex in the nitrate reduction is caused by the nitrosylation of the molybdenum species¹¹ by the reaction product, nitrite. Such NO evolution or nitrosylation to the Fe–S cluster is known¹² from periplasmic nitrate reductase isolated from *Pseudomonas*

(9) (a) Bahr, G.; Schleitzer, B. *Chem. Ber.* **1955**, *88*, 1771. (b) Bahr, G. *Angew. Chem.* **1956**, *68*, 525. (c) Stiefel, E. I.; Bennet, L. E.; Dori, Z.; Crawford, T. H.; Simo, C.; Gray, H. B. *Inorg. Chem.* **1970**, *9*, 281–286. (d) Davidson, A.; Holm, R. H. *Inorg. Synth.* **1967**, *10*, 8.

(10) Das, S. K.; Chaudhury, P. K.; Biswas, D.; Sarkar, S. *J. Am. Chem. Soc.* **1994**, *116*, 9061–9070.

(11) Majumdar, A.; Pal, K.; Sarkar, S. *J. Am. Chem. Soc.* **2006**, *128*, 4196–4197.

(12) Butler, C. S.; Charnock, J. M.; Bennett, B.; Sears, H. J.; Reilly, A. J.; Ferguson, S. J.; Garner, C. D.; Lowe, D. J.; Thomson, A. J.; Berks, B. C.; Richardson, D. J. *Biochemistry* **1999**, *38*, 9000–9012.

dentrificans. Such NO production is now known as a common feature because there are reports¹³ that nitrate reductase from plants uses nitrite generated from nitrate to produce NO.

Experimental Section

Materials and Methods. All reactions and manipulations were performed under argon atmosphere using modified Schlenk technique. CH₃CH₂SH and PhCH₂SH were obtained from Lancaster and [Et₄N][I] was obtained from Spectrochem, India. PPh₄Br and [Bu₄N][NO₃] were obtained from Alfa-Essar and Aldrich, respectively. [Et₄N][Br], Et₃N, and CH₃SO₃H were obtained from S. D. Fine Chemicals, Ltd., India. Solvents were dried and distilled by standard procedure. [Et₄N]₂[Mo^{IV}O(mnt)₂] and [PPh₄]₂[Mo^{IV}O(mnt)₂] were prepared following the process reported earlier.^{10,14,15} Infrared spectra were recorded on a Bruker Vertex 70 FT-IR spectrophotometer as pressed KBr and CsI disks. Elemental analyses for carbon, hydrogen, nitrogen, and sulfur were recorded with Perkin-Elmer 2400 microanalyser. Mass spectra (ESI, negative ion) were recorded on a Waters Micromass Q-TOF Premier mass spectrometer. Absorption spectroscopic measurements and kinetics measurements for nitrate reduction by complexes **1** and **2** were performed in a USB 2000 (Ocean Optics Inc.) UV-visible spectrophotometer equipped with fiber optics. Cyclic voltammetric measurements were made with a BASi Epsilon-EC Bioanalytical Systems, Inc. instrument. Cyclic voltammograms and differential pulse polarographs of 10⁻³ M solution of the compounds were recorded (see Supporting Information) with a glassy carbon electrode as working electrode, 0.2 M Bu₄NClO₄ as supporting electrolyte, Ag/AgCl electrode as reference electrode, and a platinum auxiliary electrode. Sample solutions were prepared in presence of PPh₃ in dichloromethane. PPh₃ was used externally to stabilize the complexes in solution. All electrochemical experiments were done under argon atmosphere at 298 K. Potentials are referenced against internal ferrocene (Fc) and are reported relative to the Ag/AgCl electrode ($E_{1/2}(\text{Fc}^+/\text{Fc}) = 0.459 \text{ V vs Ag/AgCl electrode}$).

Synthesis. [PPh₄][Mo^{IV}(PPh₃)(SCH₂CH₃)(mnt)₂].CH₂Cl₂ (**1**). To a solution of 4.28 g (4 mmol) of [PPh₄]₂[Mo^{IV}O(mnt)₂] and 10.49 g (40 mmol) of PPh₃ in 100 mL of dichloromethane at 0 °C was slowly added 1 mL of methanesulphonic acid with constant stirring. Initial green color of the solution turned bright red after 10 min, and then 1.77 mL of CH₃CH₂SH (24 mmol) was added to this solution. Stirring was continued for another 15 min at 0 °C when the solution acquired a dark violet color. Addition of petroleum ether (60–80 °C) resulted in incipient cloudiness and on standing overnight at 4 °C dark violet block shaped diffraction quality crystals separated out. These were filtered, washed with petroleum ether, and dried under inert atmosphere. Yield: 4.046 g (90%). Analysis required for C₅₃H₄₂Cl₂MoN₄P₂S₅: C, 53.65; H, 3.67; N, 4.63; S, 13.26%. Found: C, 53.75; H, 3.76; N, 4.75; S, 13.32%. Absorption spectrum (dichloromethane) λ_{max} (ϵ_{M}): 387 (6350), 512 (4920), 555 (3985) nm. IR (KBr pellet): ν 2200 (CN), 3055 (aromatic CH stretching), 724 (aromatic CH bending) cm⁻¹.

IR (CsI pellet): ν 352, 345 (Mo^{IV}-S_{dithiolene}), 326 (Mo^{IV}-S_{Et}) cm⁻¹. ³¹P NMR: δ 49.88, s. MS: $m/z = 700.908$ ([Mo^{IV}(PPh₃)-(SCH₂CH₃)(mnt)₂]¹⁻), 438.880 ([Mo^{IV}(SCH₂CH₃)(mnt)₂]¹⁻).

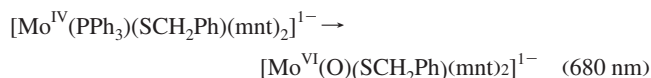
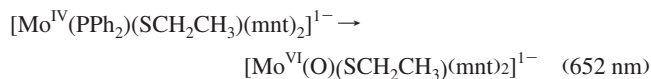
[PPh₄][Mo^{IV}(PPh₃)(SCH₂Ph)(mnt)₂] (**2**). To a solution of 4.28 g (4 mmol) of [PPh₄]₂[Mo^{IV}O(mnt)₂] and 10.49 g (40 mmol) of PPh₃ in 100 mL of dichloromethane, 1 mL of methanesulphonic acid was slowly added at 0 °C with constant stirring. The initial green color of the solution changed to bright red. After 10 min, 2.85 mL of PhCH₂SH (24 mmol) was added into this solution. Stirring was continued for another 15 min at 0 °C when the solution became dark violet. Petroleum ether (60–80 °C) was added to initiate cloudiness, and the mixture was allowed to stand overnight at 4 °C to yield dark violet block shaped diffraction quality crystals. These were filtered and washed with petroleum ether and dried under inert atmosphere. Yield: 3.96 g (90%). Required for C₅₇H₄₂MoN₄P₂S₅: C, 62.17; H, 3.84; N, 5.09; S, 14.56%. Found: C, 62.25; H, 3.92; N, 5.16; S 14.62%. Absorption spectrum (dichloromethane) λ_{max} (ϵ_{M}): 387 (5510), 512 (4375), 555 (3690) nm. IR (KBr pellet): ν 2200 (CN), 3055 (aromatic CH stretching), 724 (aromatic CH bending) cm⁻¹. IR (CsI pellet): ν 350, 343 (Mo^{IV}-S_{dithiolene}), 324 (Mo^{IV}-S_{CH₂Ph}) cm⁻¹. ³¹P NMR: δ 49.58, s. MS: $m/z = 763.068$ ([Mo^{IV}(PPh₃)(SCH₂Ph)(mnt)₂]¹⁻), 500.833 ([Mo^{IV}(SCH₂Ph)(mnt)₂]¹⁻).

[Et₄N][Mo^{IV}(PPh₃)(Br)(mnt)₂] (**3**). To a solution of 2.62 g (4 mmol) of [Et₄N]₂[Mo^{IV}O(mnt)₂], 10.49 g (40 mmol) of PPh₃ in 100 mL of dichloromethane was added 1 mL methanesulphonic acid dropwise with constant stirring at 0 °C. After the bright red solution was stirred for 10 min., 5.04 g (24 mmol) of Et₄NBr was added. Stirring was continued for another 15 min at 0 °C to get a clear red solution. The addition of petroleum ether (60–80 °C) and standing overnight at 4 °C produced reddish orange crystals that were contaminated with an oily mass. The whole mass was filtered, washed with isopropyl alcohol, followed by diethyl ether, to remove the oily part and dried in vacuum to get needle-shaped dark reddish orange diffraction quality crystals. Yield: 3.05 g (90%). Required for C₃₄H₃₅BrMoN₅PS₄: C, 48.11; H, 4.16; N, 8.25; S, 15.11%. Found: C, 48.22; H, 4.21; N, 8.31; S 15.21%. Absorption spectrum (dichloromethane) λ_{max} (ϵ_{M}): 364 (5150), 400 (5500) 489 (3275), 519 (3000) nm. IR (KBr pellet): ν 2200 (CN), 3050 (aromatic CH stretching), 730 (aromatic CH bending) cm⁻¹. ³¹P NMR: δ 49.76, s. MS: $m/z = 718.826$ ([Mo^{IV}(PPh₃)(Br)(mnt)₂]¹⁻), 456.724 ([Mo^{IV}(Br)(mnt)₂]¹⁻).

[Et₄N][Mo^{IV}(PPh₃)(I)(mnt)₂].CH₂Cl₂ (**4**). To a solution of 2.62 g (4 mmol) of [Et₄N]₂[Mo^{IV}O(mnt)₂], 10.49 g (40 mmol) of PPh₃ in 100 mL of dichloromethane at 0 °C, was added 1 mL of methanesulphonic acid dropwise with constant stirring. The solution became bright red after 10 min, and 6.17 g (24 mmol) of Et₄NI was added to this solution. Stirring was continued for another 15 min 0 °C, and the solution became dark violet in color. Petroleum ether (60 °C-80 °C) was added to the filtrate to initiate incipient cloudiness, and the mixture was allowed to stand overnight at 4 °C to form dark violet crystals that were contaminated with an oily mass. The whole mass was filtered, washed with water, followed by isopropyl alcohol and diethyl ether, to remove the oily part and dried in vacuum to get the block-shaped violet diffraction quality crystals. Yield: 3.00 g (85%). Required for C₃₅H₃₇Cl₂IMoN₅PS₄: C, 42.86; H, 3.80; N, 7.14; S, 13.08%. Found: C, 42.92; H, 3.89; N, 7.21; S 13.17%. Absorption spectrum (dichloromethane) λ_{max} (ϵ_{M}): 378 (7190), 511 (2800), 568 (2710) nm. IR (KBr pellet): ν 2200 (CN), 3050 (aromatic CH stretching), 740 (aromatic CH bending) cm⁻¹. ³¹P NMR: δ 49.16, s. MS: $m/z = 766.463$ ([Mo^{IV}(PPh₃)(I)(mnt)₂]¹⁻), 504.710 ([Mo^{IV}(I)(mnt)₂]¹⁻).

- (13) (a) Desikan, R.; Griffiths, R.; Hancock, J.; Neill, S. *Proc. Natl. Acad. Sci.* **2002**, *99*, 16314–16318. (b) Rockel, P.; Strube, F.; Rockel, A.; Wildt, J.; Kaiser, W. M. *J. Expt. Bot.* **2002**, *53*, 103–110. (c) Lamotte, O.; Courtois, C.; Barnavon, L.; Pugin, A.; Wendehenne, D. *Planta* **2005**, *221*, 1–4.
 (14) Maity, R.; Nagarajan, K.; Sarkar, S. *J. Mol. Struct.* **2003**, *656*, 169–176.
 (15) Nagarajan, K.; Joshi, H. K.; Chaudhury, P. K.; Pal, K.; Cooney, J. A.; Enemark, J. H.; Sarkar, S. *Inorg. Chem.* **2004**, *43*, 4532–4533.

Kinetics Measurements. These reactions were performed in dichloromethane solution. Electronic spectroscopic and kinetics measurements for nitrate reduction by complexes **1** and **2** were performed using a USB 2000 (Ocean Optics Inc.) UV–visible spectrophotometer equipped with fiber optics. Nitrate reduction was followed by observing the appearance of the 770 (in case of **1**) and 790 nm bands (in case of **2**). Sharp isosbestic points demonstrated that these two oxo transfer reactions proceeded cleanly in the first phase of completion of the reaction



Reaction systems contained concentrations of 1×10^{-4} M for complexes **1** and **2** with an excess substrate $[(\text{Bu}_4\text{N})(\text{NO}_3)]$ concentration in the range of $1.25\text{--}3 \times 10^{-4}$ M. For each complex, reactions were run at least three times at each substrate concentration at 25 °C under first-order conditions. Plots of $(-\ln C_t) [C_t = (\epsilon_2 C_0 - \text{OD})/(\epsilon_2 - \epsilon_1)]$, where ϵ_1 and ϵ_2 are the molar absorption coefficients of the thiolate complexes (**1** or **2**) and their oxidized species at 770 and 790 nm, respectively, versus time were linear, from which k_{obs} values were calculated at each substrate concentration. Plot of $1/k_{\text{obs}}$ versus $1/[(\text{Bu}_4\text{N})(\text{NO}_3)]$ (Lineweaver–Burk plot) yielded the V_{Max} and K_{M} values. Errors (see Supporting Information) were estimated using the EO4FDF NAG FORTRAN Library routine document.¹⁶ Because the oxidized species corresponding to complexes **1** and **2** could not be isolated because of their subsequent reaction with product nitrite, ϵ_2 values for the complexes **1** and **2** were calculated from the maximum absorbance observed at 770 and 790 nm during the reaction course with $[\text{Bu}_4\text{N}][\text{NO}_3]$ assuming full conversion.

Determination of Nitrite. Nitrite generated in the system containing $[\text{Bu}_4\text{N}][\text{NO}_3]$ and complexes **1** or **2** was measured quantitatively following a colorimetric method.¹⁷ Immediately after completion of the oxo transfer reaction, the solvent in the reaction mixture was removed under vacuum, and the residue was extracted with water. Griess reagent (1:1 mixture of 0.1% N/1-naphthylethylenediamine dihydrochloride in water and 1% sulfanilamide in 5% phosphoric acid) was added to the extract to obtain a purple solution. Absorbance at 550 nm was measured, and the concentration was calculated with the help of a standard curve made with preknown concentration of NaNO_2 . Nitrite generated in these systems corresponded to about 90% of the theoretical conversion for a complete reaction.

X-ray Structure Determinations. Suitable diffraction quality single crystals were obtained from the crystallization procedures described in each synthesis. The crystals used in the analyses were glued to glass fibers and mounted on BRUKER SMART APEX diffractometer. The instrument was equipped with CCD area detector, and data were collected using graphite-monochromated Mo K α radiation ($\lambda = 0.71069$ Å) at low temperature (100 K). Cell constants were obtained from the least-squares refinement of three-dimensional centroids through the use of CCD recording of narrow ω -rotation frames, completing almost all-reciprocal space in the stated θ range. All data were collected with SMART 5.628 (BRUKER, 2003), and were integrated with the BRUKER SAINT

program. The structure was solved using SIR97¹⁸ and refined using SHELXL-97.¹⁹ Crystal structures were viewed using ORTEP.²⁰ The space group of the compounds was determined based on the lack of systematic absence and intensity statistics. Full-matrix least-squares/difference Fourier cycles were performed which located the remaining non-hydrogen atoms. All non-hydrogen atoms were refined with anisotropic displacement parameters. Complex **1** contains one cation, one anion, and one dichloromethane in the asymmetric unit. The structure suffered from disorder of unidentified solvent (CH_2Cl_2 /petroleum ether) in the lattice, which was not included in the refinement but was taken care of by the SQUEEZE-procedure (from PLATON). The volume occupied by the solvent was 235.3 Å³, and the number of electrons per unit cell deduced by SQUEEZE was 31.8. Complexes **2** and **3** possess only one anion and one cation in their respective asymmetric units. Complex **4** contains half of a cation, half of an anion, and half of a dichloromethane molecule in its asymmetric unit. One phenyl ring of the triphenylphosphine moiety in the anion of complex **4** is disordered over two positions which were refined with free part instruction using SHELXL-97.¹⁹

Results and Discussion

Synthesis and Reactivity of Compounds. In the complex, $[\text{Mo}^{\text{IV}}\text{O}(\text{mnt})_2]^{2-}$,^{10,14} the molybdenyl group, $\{\text{Mo}^{\text{IV}}=\text{O}\}$, behaves like the carbonyl group as the $\{\text{Mo}=\text{O}\}$ double bond can easily be protonated with the addition of an acid (HX) to yield $\{\text{Mo}^{\text{IV}}(\text{OH})(\text{X})\}$ group, and when the counteranion, X, is a non-coordinating anion like methanesulfonate, the species responds to hydrolysis finally to yield the stable tris²¹ species, $[\text{Mo}^{\text{IV}}(\text{mnt})_3]^{2-}$ in 67% yield based on the molybdenum present. Its formation can be near quantitative on addition of 1 equiv of free mnt anion into the reaction medium.²² The direct formation of the bluish green tris product may be prevented once the acidification is carried out in the presence of triphenylphosphine where the initial brownish green color of the solution rapidly changed to red presumably because of the formation of the probable reaction intermediate, $\{\text{Mo}^{\text{IV}}(\text{PPh}_3)(\text{OH})(\text{mnt})_2\}$ (Figure 2). Addition of $\text{CH}_3\text{CH}_2\text{SH}$, PhCH_2SH , Et_4NBr , and Et_4NI at this stage into this red solution yielded the complexes **1–4** (Chart 1). The presence of excess PPh_3 at this stage is crucial in isolating these complexes in excellent yield because excess PPh_3 prevents the back reaction in forming the hypothetical lone hydroxo species which rapidly changed to the tris²¹ complex. Complexes **1** and **2** dissociate readily in solution generating the active pentacoordinated species, $[\text{Mo}^{\text{IV}}(\text{S-R})(\text{mnt})_2]^{1-}$ ($\text{R} = -\text{CH}_2\text{CH}_3, -\text{CH}_2\text{Ph}$), which are competent

(16) Box, G. E. P.; Hunter, W. G.; Hunter, J. S. In *Statistics for Experiments*; John Wiley & Sons: New York, 1978.

(17) Basset, J.; Denney, R. C.; Jeffery, G. H.; Mendham, J. In *Vogel's Textbook of Quantitative Chemical Analysis*; Longman Scientific and Technical: Harlow, Essex, U.K., 1989; pp 702 ff.

(18) Altomare, A.; Burla, M. C.; Camalli, M.; Cascarano, G. L.; Giacovazzo, C.; Guagliardi, A.; Moliterni, A. G. G.; Polidori, G.; Spagna, R. *J. Appl. Crystallogr.* **1999**, *32*, 115–119.

(19) Sheldrick, G. M. *SHELX97, Programs for Crystal Structure Analysis*, (release 97–2); University of Göttingen: Göttingen, Germany, 1997.

(20) Farrugia, L. J. *J. Appl. Crystallogr.* **1997**, *30*, 565.

(21) (a) Brown, G. F.; Stiefel, E. I. *Inorg. Chem.* **1973**, *12*, 2140–2147. (b) Xu, H.-Wu.; Chen, Z.-N.; Wu, J.-G. *Acta Crystallogr. E* **2002**, *58*, m631. (c) Formichev, D. V.; Lim, B. S.; Holm, R. H. *Inorg. Chem.* **2001**, *40*, 645–654. (d) Wang, K.; McConnachie, J. M.; Stiefel, E. I. *Inorg. Chem.* **1999**, *38*, 4334–4341. (e) Matsubayashi, G.; Douki, K.; Tamura, H.; Nakano, M.; Mori, W. *Inorg. Chem.* **1993**, *32*, 5990–5996. (f) Draganjac, M.; Coucouvanis, D. *J. Am. Chem. Soc.* **1983**, *105*, 139–140.

(22) Das, S. K.; Biswas, D.; Maiti, R.; Sarkar, S. *J. Am. Chem. Soc.* **1996**, *118*, 1387–1397.

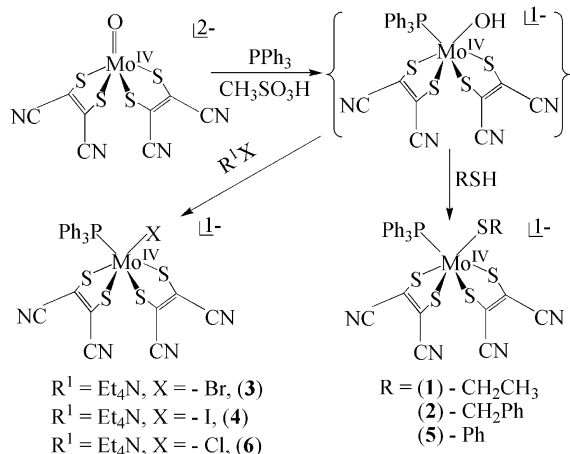


Figure 2. Schematic representation for the synthesis of complexes 1–6.

to reduce nitrate to nitrite. The formation of nitrite from nitrate in such reaction can be confirmed by Griess's reagent with blank tests as controls in the absence of **1** or **2**. Reversible dissociation of triphenylphosphine (PPh_3) from the complexes **1** and **2** has been monitored by ^{31}P NMR spectroscopy (see Supporting Information). With time, the peak intensity (δ 49.89, s) due to PPh_3 bound to molybdenum(IV) center (**1**) decreases with the concomitant increase of the peak intensity (δ -8.16, s) because of dissociated free PPh_3 . Reversibility of the triphenylphosphine dissociation was confirmed by the addition of free PPh_3 in the solution, while monitoring the ^{31}P NMR spectroscopy which restored the maximum intensity of the δ 49.89 peak responsible for the PPh_3 bound to molybdenum(IV) (**1**). Compounds **3**, **4**, and **6** (Chart 1) also dissociate in solution, but the dissociation was found to be very slow: no appreciable dissociation up to 2 h was noticed. With time, these are slowly converted to the thermodynamically stable tris 21 $[\text{Mo}^{\text{IV}}(\text{mnt})_3]^{2-}$ complex in dichloromethane solution (see Supporting Information). Complex **5** is rapidly converted to **3**, **4**, and **6** with Et_4NBr , Et_4NI , and Et_4NCl , respectively. Even the presence of PhCH_2Br is sufficient, albeit slowly, to trigger the conversion of **5** to **3** (see Supporting Information), whereas the thiolate groups in complexes **1** and **2** cannot be substituted even in the presence of a large excess of respective halides. These observations showed the stability of the aliphatic thiolato coordination in the reactive species to interact with the nitrate ion.

X-Ray Structure Description. All four complexes (**1–4**) are characterized by X-ray structure determination. All the four complexes are isostructural, and structures of **1** and **4** are shown in Figure 3 (see Supporting Information for the structures of **2** and **3**), and the leading structural parameters are collected in Table 1. The selected bond distances are presented in Table 2. For the most part, these parameters are in good agreement with the other related molybdenum bis(dithiolene) complexes.^{10,11,14,15} The ranges of mean C–C and S–C bond distances are 1.33–1.34 and 1.73–1.79 Å, respectively, which are sufficiently close to the typical bond lengths ($\text{sp}^2\text{C}=\text{C}(\text{sp}^2) = 1.331(9)$ Å and $\text{S}-\text{C}(\text{sp}^2) = 1.75(2)$ Å to establish the ligand mnt^9 as a classical ene-1,2-dithiolate,

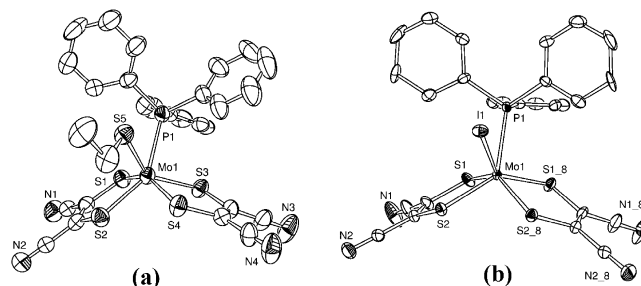
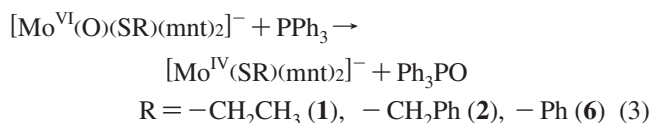
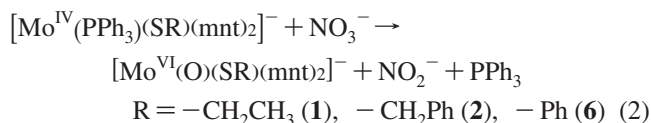


Figure 3. Structure (ORTEP view) of anions of **1** (a) and **4** (b) showing 50% probability thermal ellipsoids with atom labeling scheme. Hydrogen atoms are omitted for clarity.

as observed in other reported bis(dithiolene) molybdenum complexes.^{7,10,11} There is very little variation in the Mo–P bond distance within the series (**1–4**) and the structurally similar complexes (**5** and **6**) (Chart 1). The Mo–P bond distance is longest (2.590 Å) in the case of complex **2** and shortest (2.538 Å) in the case of complex **5**. Complex **1** exhibits slightly longer Mo–S(thiolate) bond distance (2.367 Å) than in the case of complex **2** (2.338 Å) or complex **5** (2.336 Å). The Mo–S(thiolate) bond distance in complexes **1**, **2**, and **5** are quite longer than that in the related molybdenum bis(dithiolene) complexes (2.312^{7b,c} and 2.320 Å)^{7a} but appreciably shorter than that reported (2.469 Å) in the case of another related molybdenum bis(dithiolene) complex, $[\text{Et}_4\text{N}][\text{Mo}^{\text{IV}}(\text{CO})(\text{SPh})(\text{S}_2\text{C}_2\text{Me}_2)_2]$.^{7a} In complexes **1**, **2**, and **5**, the distance between thiolate sulfur atom and phosphorus atom of triphenylphosphine moiety ranges from 3.066 (complex **1**) to 3.098 Å (complex **5**), while the Mo–S(thiolate)–P angle ranges from 76.29° (complex **1**) to 77.00° (complex **2**). Mo–X bond distances are 2.626 (X = Br) and 2.834 Å (X = I) in complexes **3** and **4**, respectively. Displacement of Mo atom from the S_4 (dithiolene sulfur) mean plane (see Table 2) varies from 0.815 (in complex **3**) to 0.857 Å (in complex **2**).

Oxo Transfer Reaction with Nitrate. The reaction of nitrate with $([\text{Bu}_4\text{N}][\text{NO}_3])$ as the oxo-donor substrate was found to be successful only with two complexes (**1** and **2**) within the series (**1–4**). Complexes **1** and **2** individually react with $[\text{Bu}_4\text{N}][\text{NO}_3]$ in dichloromethane medium at varying rates. When such reactions with complexes **1** and **2** are monitored by ^{31}P NMR spectroscopy with $[\text{Bu}_4\text{N}][\text{NO}_3]$ as substrate in 1:2 molar ratio, only one signal appeared¹¹ (other than the signal at 20.50 ppm corresponding to PPh_4^+) at 24.97 ppm corresponding to triphenylphosphine oxide (Ph_3PO) as shown in the eqs 2 and 3.



The oxidized species, $\{[\text{Mo}^{\text{VI}}(\text{O})(\text{SR})(\text{mnt})_2]^{-}\}$, produced through the reduction of nitrate (eq 2) is reduced back (eq

Table 1. Crystallographic Data^a for Complexes 1–4

complexes	1	2	3	4
formula	C ₃₃ H ₄₂ Cl ₂ MoN ₄ P ₂ S ₅	C ₅₇ H ₄₂ MoN ₄ P ₂ S ₅	C ₃₄ H ₃₅ BrMoN ₅ PS ₄	C ₃₅ H ₃₇ Cl ₂ IMoN ₅ PS ₄
fw	1124.04	1101.18	848.76	980.69
cryst syst	triclinic	monoclinic	orthorhombic	orthorhombic
space group	<i>P</i> 1	<i>P</i> 2 ₁ / <i>n</i>	<i>Pna</i> 2 ₁	<i>Pnma</i>
<i>T</i> (K)	100	100	100	100
<i>Z</i>	2	4	4	4
<i>a</i> (Å)	12.645(5)	13.976(5)	13.275(5)	13.616(5)
<i>b</i> (Å)	14.499(5)	20.679(5)	18.470(5)	15.386(5)
<i>c</i> (Å)	16.709(5)	19.302(5)	15.227(5)	18.900(5)
α (deg)	113.494(5)	90	90	90
β (deg)	93.162(5)	109.979(5)	90	90
γ (deg)	91.779(5)	90	90	90
<i>V</i> (Å ³)	2800.5(17)	5243(3)	3734(2)	3960(2)
<i>d</i> _{calcd} (g/cm ³)	1.333	1.395	1.510	1.645
μ (mm ⁻¹)	0.611	0.552	1.719	1.530
θ range (deg)	2.16–28.77	2.20–28.39	2.04–28.29	2.15–28.31
GOF (<i>F</i> ²)	0.909	1.070	1.116	1.043
R1 ^b (wR2) ^c (%)	0.0736 (0.1628)	0.0869 (0.1517)	0.0639 (0.1121)	0.0506 (0.1139)

^a Mo Kα radiation. ^b R1 = $\sum |F_o - F_c| / \sum F_o$. ^c wR2 = $\{\sum [w(F_o^2 - F_c^2)^2] / \sum [w(F_o^2)^2]\}^{1/2}$.

Table 2. Selected Bond Distances (Å) for Complexes 1–4

distances	1	2	3	4
Mo(1)–P(1) _{PPh₃}	2.59(2)	2.59(2)	2.54(2)	2.55(2)
Mo(1)–S(5) _{thiolate}	2.37(2)	2.34(2)		
displacement of Mo(1) from S ₄ (dithiolene sulfur) mean plane	0.841	0.857	0.815	0.817

3) to $\{[\text{Mo}^{\text{IV}}(\text{SR})(\text{mnt})_2]^{1-}\}$ (R = –SCH₂CH₃, –SCH₂Ph) with concomitant formation of triphenylphosphine oxide (Ph₃PO). Appearance of only one signal corresponding to Ph₃PO indicated the reaction of nitrate with **1** and **2** to be almost quantitative. Nitrate reduction by complexes **1** and **2** in dichloromethane solution were monitored by UV–vis spectroscopy (Figure 4 for **1**, see Supporting Information for **2**). During the progress of the reaction, the intensity of the parent absorption band at 512 nm along with the shoulder at 555 nm started to decrease with time. Complex **1** showed full development of a new band at 770 nm within 1.5 min (Figure 4), whereas in the case of complex **2**, complete development of a new band at 790 nm occurred within 3 min (see Supporting Information). Appearance of tight isosbestic points at 652 nm (Complex **1**, Figure 4) and 680

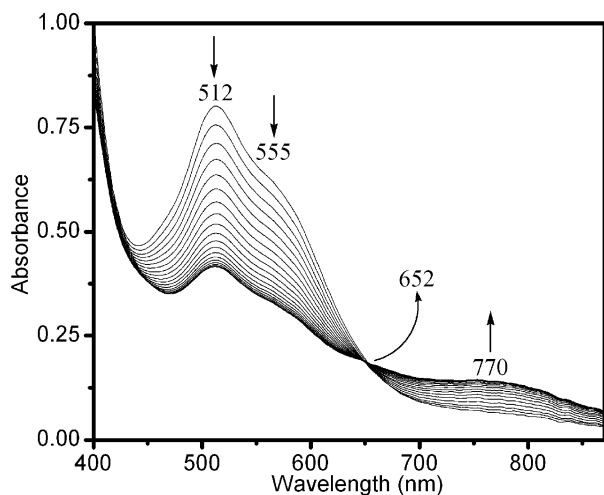


Figure 4. Spectrophotometric monitoring of the reaction of $[\text{PPh}_4][\text{Mo}^{\text{IV}}(\text{PPh}_3)(\text{SCH}_2\text{CH}_3)(\text{mnt})_2] \cdot \text{CH}_2\text{Cl}_2$ (**1**) (2×10^{-4} M) with $[\text{Bu}_4\text{N}][\text{NO}_3]$ (10×10^{-4} M) in dichloromethane. Total time = 90 s. Scan rate = 5 s/scan.

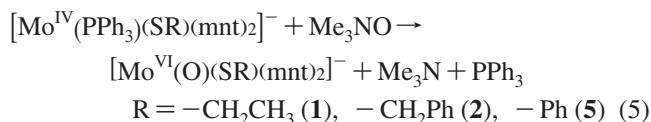
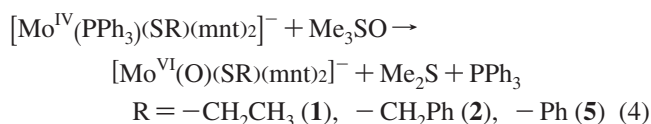
nm (Complex **2**, see Supporting Information) indicated clean reduction of nitrate in both the cases. The oxidized species $\{[\text{Mo}^{\text{VI}}(\text{O})(\text{SR})(\text{mnt})_2]^{1-}\}$, despite numerous attempts, could not be isolated so far. This is because of its participation in the successive reactions with the nitrite produced in the oxo transfer reaction. The oxidized species once formed slowly started to change into another species using the available nitrite present in the medium. It was found that the concentration of the nitrite produced steadily increased during the first 1.5 and 3 min (in **1** and **2**, respectively) in these oxo transfer reactions, but on standing for more than 10 min, the concentration of the nitrite started decreasing in the solution and after an hour the available concentration of nitrite from the solution decreased appreciably. Routine workup procedure of the resultant solution on standing yielded known orange-brown species²³ $[\text{Mo}^{\text{IV}}(\text{NO})_2(\text{mnt})_2]^{2-}$. Characterization of this species with the aid of IR spectroscopy (ν_{NO} , KBr disk 1730 and 1625 cm^{-1}) present as the final molybdenum product¹¹ helped in explaining our inability in isolating the oxidized molybdenum species. Sulfamic acid being insoluble in dichloromethane could not be used to scavenge⁶ the nitrite ion produced in the oxo-transfer reaction to protect the oxidized species formed to participate further reaction with nitrite ion. Interestingly, periplasmic nitrate reductase from *P. denitrificans*, while reacting with nitrate as substrate was shown to produce NO and part of the Fe–S proteins was shown to be nitrosylated with the formation of {FeNO} moiety.¹² Further, groups of plant nitrate reductase have been shown to use nitrite to produce NO.¹³ The nitrosylation of molybdenum in the model systems may occur because of the absence of protein which may control the gate of substrate and product for proper channelization to control local concentration around the active metal center for the necessary enzymatic reaction. The addition of nitrate to the solution of **3**, **4**, and **6** led to formation of the tris²¹ complex almost instantaneously, whereas this conversion in the absence of nitrate or any other

(23) (a) McCleverty, J. A. *Prog. Inorg. Chem.* **1968**, *10*, 49. (b) Connelly, N. G.; Locke, J.; McCleverty, J. A.; Phipps, D. A.; Ratcliff, B. *Inorg. Chem.* **1970**, *9*, 278–280.

reagent is relatively slow (see Supporting Information for 3 and 4). Monitoring these reactions by ^{31}P NMR clearly showed that the presence of nitrate or other ligands completely dissociated the bound PPh_3 from the molybdenum, whereas in the absence of any external ion or ligand there remained an equilibrium between the bound and unbound PPh_3 , and in the presence of excess of PPh_3 , the hexacoordinated complexes became stable for a longer time. The addition of nitrate influenced the release of bound PPh_3 to produce free pentacoordinated species like $[\text{Mo}^{\text{IV}}(\text{X})(\text{mnt})_2]^{1-}$ ($\text{X} = -\text{Br}$ (3), $-\text{I}$ (4), and $-\text{Cl}$ (6)) which even on binding of nitrate at the released site are not capable to reduce nitrate and hence are rapidly converted to the thermodynamically stable tris 21 complex. These results clearly indicate the indispensable role of thiolate ligation in the synthetic model complexes (1, 2, and 5) in their response to show oxo-transfer reaction similar to native dissimilatory nitrate reductase.

Oxo Transfer Reaction with DMSO and TMANO.

Complexes 1, 2, and 5 are found to reduce DMSO, as well as TMANO as shown in eqs 4 and 5. The oxidized species, $\{[\text{Mo}^{\text{VI}}(\text{O})(\text{SR})(\text{mnt})_2]^{1-}\}$, produced through the reactions (eq 4 and 5) are reduced back to



$\{[\text{Mo}^{\text{IV}}(\text{SR})(\text{mnt})_2]^{1-}\}$ ($\text{R} = -\text{SCH}_2\text{CH}_3$, $-\text{SCH}_2\text{Ph}$, $-\text{SPh}$) according to eq 3, with concomitant formation of triphenylphosphine oxide (Ph_3PO). This was confirmed by the observation that when the reaction with complexes 1, 2, or 5 were monitored by ^{31}P NMR spectroscopy with DMSO or TMANO as substrate in 1: 2.5 molar ratio, a signal appeared at 24.97 ppm corresponding to triphenylphosphine oxide (Ph_3PO). It is known that in the absence of any catalyst, DMSO and Ph_3P do not react for at least 1 h even at 189 $^{\circ}\text{C}$. 24 Also it is checked that TMANO and Ph_3P together (1:1 mole ratio) in dichloromethane at ambient condition (25 $^{\circ}\text{C}$) did not produce any identifiable Ph_3PO up to a period of 1 h. Therefore the presence of Ph_3PO in the reaction mixture strongly supports that the starting species participated in oxo transfer reaction with DMSO (or TMANO) resulting its oxidation which in turn was reduced by the partially released Ph_3P . Along with the presence of 24.97 ppm signal for Ph_3PO and 20.50 ppm signal for PPh_4^+ , two ^{31}P signals characteristic of the Mo^{IV} bound PPh_3 and free PPh_3 were observed in the case of complexes 1, 2, and 5 when allowed to react with DMSO (or TMANO). The presence of Mo^{IV} -bound PPh_3 and free PPh_3 suggested that reactions 4 and 5 are not complete with DMSO and TMANO as substrates respectively. DMSO (or TMANO) reduction by these complexes in dichloromethane solution was monitored by

UV-vis spectroscopy with 1: 2.5 molar ratios of complexes (see Supporting Information). During the progress of the reaction with DMSO, complexes 1 and 2 showed gradual decrease in the intensity of the absorption band at 512 nm along with the shoulder at 555 nm with concomitant development of a new band at 770 and 790 nm, respectively (see Supporting Information). Complex 5 exhibited gradual decrease of the intense absorption band at 515 nm, along with the shoulder at 570 nm with concomitant development of the 770 nm band (see Supporting Information). The progress of reaction with TMANO as substrate showed similar behavior for these complexes. These reactions are not clean and are associated with uncharacterized side reactions leading ultimately to the formation of "tris" species. Interestingly with DMSO (or TMANO) reaction a residual purple color quite similar to the parent complex (1, 2, and 5) is retained even at the end of the maximum development of the new band at 770 and 790 nm. On the basis of the ^{31}P NMR data for Ph_3PO in comparison with the nitrate reducing systems, an estimated 15–20% conversion was found in case of oxo transfer reaction with TMANO or DMSO. DMSO reduction was also confirmed by passing a slow stream of dinitrogen through the reaction mixture to drive out the formed dimethylsulfide first through a trap and then through an aqueous solution of HgCl_2 , leading to the white precipitation of $(\text{Me}_2\text{S})_2(\text{HgCl}_2)_3$. Quantification of this solid when washed and dried indicated roughly 15% conversion. When 1 or 2 (also 5) in solution was treated with dimethylsulfide (DMS), the color of the solution changed immediately. ^{31}P NMR spectroscopic measurements of 1 and 2 (also 5) in dichloromethane with excess DMS showed complete displacement of PPh_3 ($\delta -8.16$ ppm, s) by dimethylsulfide. The coordination of DMS in native DMSOR has been reported. 25 In the present case, the binding of DMS at $\text{Mo}(\text{IV})$ site can be observed by monitoring the changes in the electronic spectrum of the starting complex upon addition of DMS (see Supporting Information). However, such coordinated species though relatively stable but cannot be isolated in the solid state as it slowly changes to tris 21 complex (see Supporting Information). Reaction of DMSO with complexes 1 and 2 in presence of DMS shows partial development of the absorbance bands characteristic of tris species (see Supporting Information). This chemistry is simple as excess DMS replaced PPh_3 and formed a new passive complex where the DMS coordination competes with nitrate coordination.

Kinetics of Nitrate Reduction. Kinetics measurements for the reduction of nitrate by the complexes 1 and 2 revealed that the reactions follow Michaelis–Menten kinetics. The Michaelis plots for the reduction of nitrate by the complex 1 is shown along with the Lineweaver–Burk plots as inset in Figure 5 (see Supporting Information for 2). Kinetics results are presented in Table 3. Nitrate reduction by the complex 1 is much faster than that with complex 2 or complex 5 reported earlier. 11 Ratio of V_{Max} calculated for

(25) (a) Bray, R. C.; Adams, B.; Smith, A. T.; Richards, R. L.; Lowe, D. J.; Bailey, S. *Biochemistry* **2001**, *40*, 9810–9820. (b) Adams, B.; Smith, A. T.; Bailey, S.; McEwan, A. G.; Bray, R. C. *Biochemistry* **1999**, *38*, 8501–8511.

(24) Szmant, H. E.; Cox, O. *J. Org. Chem.* **1966**, *31*, 1595.

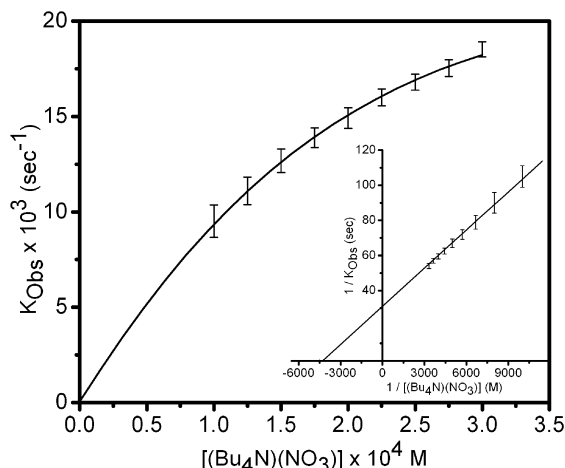


Figure 5. Dependence of the rate of reaction of $[\text{PPh}_4][\text{Mo}^{\text{IV}}(-\text{PPh}_3)(\text{SCH}_2\text{CH}_3)(\text{mnt})_2] \cdot \text{CH}_2\text{Cl}_2$ (**1**) with 1–3 equiv of $(\text{Bu}_4\text{N})(\text{NO}_3)$ in dichloromethane at 25 °C on $[(\text{Bu}_4\text{N})(\text{NO}_3)]$. Inset: the corresponding double reciprocal plot.

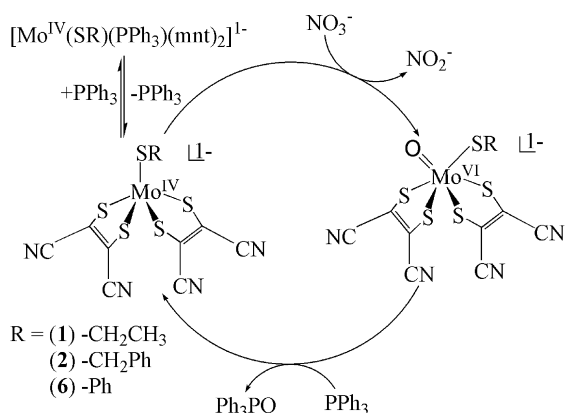
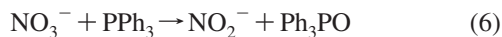


Figure 6. Catalytic cycle for nitrate reduction using $\{[\text{Mo}^{\text{IV}}(\text{SR})(\text{mnt})_2]^{1-}\}$ as the active catalyst and PPh_3 as the reductant of its putative oxidized form $\{[\text{Mo}^{\text{VI}}(\text{O})(\text{SR})(\text{mnt})_2]^{1-}\}$.

complex **1** to that calculated for complexes **2** and **5** are 4.48 and 7.68, respectively.

Catalysis of Oxo Transfer. It has been possible to couple reaction 2 and 3, with the result that the nitrate reduction (eq 6) can be made catalytic with the use of PPh_3 to regenerate the reactive pentacoordinated $\text{Mo}(\text{IV})$ complex. The catalytic cycle involving $[\text{Bu}_4\text{N}][\text{NO}_3]$ and PPh_3 as the



oxidizing and reducing substrate, respectively, is established as shown in Figure 6. The initiation of the reaction starts on the dissociation of PPh_3 from the thiolato complexes. PPh_3 recovered and Ph_3PO produced within a minute of reaction were confirmed by isolating, purifying, and checking melting points (80 and 152 °C, respectively) and by ^{31}P NMR spectroscopy (-8.16 and 24.97 ppm compared with commercial PPh_3 and Ph_3PO , respectively).¹¹ Suitable controls demonstrated no reaction between nitrate and PPh_3 (1:1 mol ratio, 25 °C, 1 h) in the absence of these thiolato complexes as catalyst. On the basis of nitrite produced (measured by standard colorimetric method), PPh_3 recovered, and Ph_3PO produced, the turnover numbers (TON) for such reactions were found out to be 10 and 40 $\text{mmol}^{-1} \text{s}^{-1}$ for complexes

1 and **2**, respectively. The low turnover number for **1** compared to that for **2** or that obtained earlier with **5** ($\text{TON} = 50 \text{ mmol}^{-1} \text{s}^{-1}$)¹¹ is the result of the formation of the oxidized species, $\{[\text{Mo}^{\text{VI}}(\text{O})(\text{SR})(\text{mnt})_2]^{1-}\}$, at a much faster rate with **1** compared with that with **2** or **5**, and therefore, a large extent of the oxidized product is consumed by competing nitrosylating reactions by the generated product nitrite prior to its reaction with PPh_3 to form Ph_3PO .

Structural Comparison of the Synthesized Complexes with the Native Active Site. Structural environment around the active site normally tunes the activity of the central atom to interact with the substrate and govern the follow-up reactions. An attempt has been made to compare the structures of the synthesized complexes (**1–6**) with that of the oxidized state of the active site for native NiR^3 (see Supporting Information for superposed structures and corresponding dihedral angles between the dithiolene planes). It was found that the dithiolene planes of synthesized thiolate (**1**, **2**, and **5**) complexes and native active site come closer when traveling from complex **5** to **2** to **1**, and the distorted octahedral geometry of the complexes became closer to the trigonal prismatic geometry of the native active site. Moreover the planes became more parallel when traveling from complex **5** to **2** to **1**, and the best match within the thiolate series was found with complex **1**. In spite of the “dithiolene fold angle”²⁶ effect, which does not allow matching of the oxidized (VI) and reduced (IV) bis(dithiolene) Mo species exactly, the structural fitting of the two dithiolene planes with the native active site can be correlated with the reactivity. A close analysis would require the availability of the structural data from the identical oxidation state of the model and native systems.

One can sum up that the active pentacoordinated model complex allowed the substrate nitrate to bind to the site vacated by PPh_3 , whereby the all important oxo transfer reaction occurred. The reactivity of the synthesized complexes followed a set pattern comparing their redox potential data (see Table 4). The reactive thiolato species showed a gradual decrease in the E_{pa} potential (CV and DPP) from complex **5** to **2** to **1**, indicating that the molybdenum center became more and more prone to oxidation (see Supporting Information for cyclic voltametric traces and differential pulse polarographs). We observed a decade ago²² that the redox potential value measured for the active complex or the active enzyme (E) can not reflect in any way its capability to respond to a redox reaction when such reaction required the formation of an enzyme–substrate complex (ES). For any atom-transfer reaction obeying Michaelis–Menten complexation, it is the thermodynamics of this complex (ES) which should be counted for its transformation to E’P (enzyme–product) reaction. However, the E_{pa} data for **1** showed that it is the easiest one to oxidize among the thiolate series, which in reality also exhibited best in its desired reaction for the reduction of nitrate. It should be noted that the

(26) (a) Joshi, H. K.; Cooney, J. A.; Inscore, F. E.; Gruhn, N. E.; Lichtenberger, D. L.; Enemark, J. H. *Proc. Natl. Acad. Sci.* **2003**, *100*, 3719–3724. (b) Lauher, J. W.; Hoffmann, R. *J. Am. Chem. Soc.* **1976**, *98*, 1729–1742.

Table 3. Kinetics Results for Nitrate Reduction by Complexes **1**, **2**, and **5**

complexes	K_M^a	V_{Max}^b
[PPh ₄][Mo ^{IV} (PPh ₃)(SCH ₂ CH ₃)(mnt) ₂]·CH ₂ Cl ₂ (1)	2.3×10^{-4} M	3.2×10^{-2} s ⁻¹
[PPh ₄][Mo ^{IV} (PPh ₃)(SCH ₂ Ph)(mnt) ₂] (2)	1.4×10^{-4} M	7.1×10^{-3} s ⁻¹
[Et ₄ N][Mo ^{IV} (PPh ₃)(SPh)(mnt) ₂]·CH ₂ Cl ₂ (5) ¹¹	4.3×10^{-4} M	4.2×10^{-3} s ⁻¹

^a K_M , kinetically determined Michaelis constant. ^b V_{Max} , maximum velocity that can be achieved.

Table 4. Redox Potentials (Oxidation Region Only) for Complexes **1–6**

complexes	E_{pa}^i (V) ^a	E (V) from DPP
1	0.698	0.689
2	0.715	0.702
5 ¹¹	0.750	0.769
3	0.900	0.887
4	0.869	0.853
6 ¹¹	0.920	0.876

^a i, irreversible.

electrochemical measurements were carried out by addition of excess PPh₃ into the solution to prevent decomposition of these complexes, and therefore, the observed electrochemistry is related to the PPh₃-bound inactive forms of the hexacoordinated species, and the electrochemical data are by no means related to those of the active pentacoordinated species. However, from the structural geometry point of view, the PPh₃ attached complexes may mimic NO₃⁻ bound state of the precursor complex (ES type) ready for oxo transfer reaction, and in that sense, the electrochemical data may be meaningful. A detailed energy level calculation of these systems is under progress to understand the electronic populations.

Relation to Enzyme. The present work provides a detailed study of some analogue systems of nitrate reductase for the reduction of biologically relevant substrate, nitrate. These complexes possess an axial thiolate ligand which very closely simulates cysteinyl coordination in dissimilatory nitrate reductase from *Desulfovibrio desulfuricans*. The analogue systems (**1**, **2**, and **5**) reduce nitrate, and the reaction follows Michaelis–Menten kinetics, similar to the native enzyme. As with other members of this family, there has been little mechanistic work on dissimilatory nitrate reductase,¹ although the steady-state kinetics behavior has been examined in case of the dissimilatory nitrate reductase from *Escherichia coli*. Using ubiquinol as electron donor, the intact enzyme is found to operate via a ping-pong mechanism, exhibiting the following kinetics parameters: $k_{cat} = 7.2$ s⁻¹, $K_M^{ubiquinol} = 78$ μM, $K_M^{nitrate} = 2$ μM, and $k_{cat}/K_M^{nitrate} = 5 \times 10^6$ M⁻¹ s⁻¹.²⁷

When these values are compared with that of the analogue systems (Table 3) discussed here (**1** and **2**) and earlier (**5**),¹¹ the conclusion is inescapable that in terms of first-order kinetics parameters, the native reduced enzyme systems are orders of magnitude more reactive than the model compounds **1**, **2**, and **5**. However, when reduced viologen dyes are used as the reducing substrate, the K_M value of 200 μM²⁸ was observed for soluble NarGH catalytic dimer of nitrate reductase, which is surprisingly close to the K_M values

obtained from these model complexes. The fastest reduction of nitrate in the synthetic series occurred with **1** containing ethanethiolate coordination to molybdenum (IV). Ethanethiol (CH₃CH₂SH) being a simple aliphatic thiol without any kind of imposed steric bulk^{7,8} resembles cysteinyl coordination and therefore established complex **1** to be the closest model system analogous to the active site of dissimilatory nitrate reductase from *Desulfovibrio desulfuricans*. Complexes **1**, **2**, and **5** are found to be reluctant to reduce DMSO because of product inhibition, and such inhibitory reactions are well-known under the feedback (regulatory) enzymes. Interestingly nitrate reductases from different sources are shown to reduce nitrate beyond nitrite with the production of NO.¹³ The inability of isolating the oxidized molybdenum product was shown to be caused by a similar reaction of the produced nitrite with the oxidized species to nitrosylate the molybdenum complex to known [Mo(NO)₂(mnt)₂]²⁻. It is to be noted that the starting reduced complexes are also capable of consuming nitrite slowly as found separately and in the presence of excess of PPh₃. The competitive reactivity of reduction of oxidized complex by PPh₃, nitrosylations of the oxidized and starting complexes by nitrite, and also the reaction between PPh₃ and any formed NO are the possible participating reactions. At the initial stage of the reaction the reduction of nitrate to nitrite is dominant and unique enough to respond to the reaction similar to NiR. The corresponding phenolate- and selenothiolate-substituted complexes are yet to be fully characterized which would have been the best systems to testify selectivity of the thiolate ligand in relevance to other molybdoenzymes.

Acknowledgment. A.M. and K.P. gratefully acknowledge predoctoral fellowships from the CSIR, New Delhi, and S.S. thanks DST, New Delhi, for funding the project. A.M. thanks Dr. P. K. Chaudhuri, Pune University, India, for useful discussions regarding kinetics experiments.

Supporting Information Available: ORTEP figures for the structures of **2** and **3**, kinetic plot of nitrate reduction reaction by **2**, ³¹P NMR spectroscopic monitoring of PPh₃ dissociation for complex **1** and **2**, UV–vis spectroscopic monitoring of reactivity (reaction of **2** with nitrate, TMANO and DMSO reduction by complexes **1**, **2**, and **5**, reaction of **1** with DMSO in presence of DMS, conversion of in situ generated [Mo^{IV}(DMS)(SR)(mnt)₂]¹⁻ complexes (**2**, R = -CH₂Ph; **5**, R = -Ph) to tris complex, tris formation reaction of complexes **3** and **4**, conversion of complex **5** to complex **3** with PhCH₂Br), cyclic voltametric traces and differential pulse polarographs, errors in kinetics experiments, and crystallographic data (in CIF format) for the complexes **1–4** and structural superposition for the complexes **1–6**. This material is available free of charge via the Internet at <http://pubs.acs.org>.

IC7024268

(27) Morpeth, F. F.; Boxer, D. H. *Biochemistry*. **1985**, *24*, 40.

(28) Buc, J.; Santini, C.-L.; Blasco, F.; Giordani, R.; Cardena, M. L.; Chippaux, M.; Cornish-Bowden, A.; Giordano, G. *Eur. J. Biochem.* **1995**, *234*, 766.